High-Level ab Initio Calculations on the Intramolecular Hydrogen Bond in Thiomalonaldehyde

Leticia González, Otilia Mó,* and Manuel Yáñez

Departamento de Química, C-9, Universidad Autónoma de Madrid, Cantoblanco, 28049-Madrid, Spain

Received: February 27, 1997; In Final Form: September 12, 1997[⊗]

High-level ab initio calculations, in the framework of the G2(MP2) theory, have been carried out on the different tautomers of thiomalonaldehyde (**TMA**). These calculations are compared with those obtained using density functional theory methods, namely B3LYP, with extended basis sets. In general the enethiol tautomers of **TMA** are 5−10 kcal/mol more stable than the corresponding enol analogues, with the only exception being the *Z*-enol (**E1**) and the *Z*-enethiol (**T1**) hydrogen-bonded species, which are the global minima of both series. At the G2(MP2) level both tautomers are nearly degenerate, the enethiol **T1** being 0.2 kcal/mol more stable than the enol **E1**. Electron correlation effects stabilize preferentially the enol form, while the ZPE corrections go in the opposite direction, due essentially to the differences between S−H and O−H stretching frequencies. As a consequence, when the hydrogen atom involved in the intramolecular hydrogen bond (IHB) of both tautomers is replaced by deuterium, the stability order is reversed and **E1** is predicted to be more stable than **T1**. An analysis of these IHBs in terms of the topological characteristics of the electron charge density and of the shifts of the S−H and O−H vibrational frequencies reveals that the HB in **E1** is much stronger than in **T1**. The existence of this IHB results in an increase of the electron delocalization which enhances the stability of tautomer **E1**. At the G2(MP2) level two open-chain rotamers, namely **T4** and **T7**, are predicted to be within an energy gap smaller than 0.5 kcal/mol with respect to the global minimum. The use of continuum and discrete−continuum models indicates that both open-chain enethiols and enols are significantly stabilized by solute−solvent interactions, and they should predominate in aqueous solution. B3LYP/6-311+G(3df,2p) relative stabilities are in excellent agreement with G2(MP2) values.

Introduction

Hydrogen bonding is one of the most important concepts in chemistry because it is crucial to understand many different interactions both in the gas phase and in condensed media.[1] A particular subset is represented by the intramolecular hydrogen bonds (IHBs), where two ends of the same molecule interact, resulting in a ringlike structure. A great deal of effort was devoted to the investigation of strong IHBs[2] such as the one present in malonaldehyde[3] or in tropolone,[4] where the two atoms that behave as the proton donor and the proton acceptor are highly electronegative. However much less attention was paid to systems where the two heavy atoms involved in the bonding present quite different electronegativities, such as oxygen and sulfur. Thiomalonaldehyde (**TMA**) constitutes a good example, where IHBs of both OH···S and SH···O types are involved in the enol−enethiol equilibrium. This system was the subject of some controversy regarding the strength of its IHB, which for the *Z*-enol tautomer was estimated to be about 6 kcal/mol stronger than that present in malonaldehyde.[5,6] A more recent study by Craw and Bacskay[7] reduced drastically this first estimation, and the IHB in the *Z*-enol form of **TMA** was found to be about 1 kcal/mol weaker than that in malonaldehyde. These very different estimations point out an additional problem inherent to IHBs, which is related to the difficulty of defining a reference structure where the HB is absent, but where the electronic structure closely resembles that of the hydrogen-bonded molecule. Another problem associated with this system is the relative stabilities of both the *Z*-enol (**E1**) and the *Z*-enethiol (**T1**) tautomers, which are predicted to be almost degenerate. Two different estimations, based on ab initio calculations, have been reported in the literature[5−7]so far. At the MP2/6-31G(d,p)//HF/3-21G + ZPE level the *Z*-enol form was found to be 2.1 kJ/mol more stable than the *Z*-thienol one. At the MP2/TZP//HF/TZP level this energy gap becomes 7.8 kJ/mol. The sizable difference between both estimations clearly shows the importance of the ZPE corrections in this particular problem.

Since we are dealing with quite small energy differences and the theoretical treatments mentioned above were based on HF optimized structures and final MP2 energies, it seems advisable to reinvestigate this problem using theoretical techniques which ensure a higher accuracy. Hence, the main goal of this paper is to study the relative stabilities of the HBs in **TMA** and its thienol tautomer using high-level ab initio calculations. This would imply also the study of the relative stabilities of all possible enol (**E1**−**8**) and enethiol (**T1**−**8**) tautomers that, as we shall show later on, may compete in stability with the two structures that present an IHB. For the sake of completeness we have also included in our study the corresponding diketo structures (**K1**−**4**). We have also obtained the corresponding proton-transfer potential energy curve connecting the *Z*-enol (**E1**) and the *Z*-enethiol (**T1**) forms, and we have investigated the possible influence of the deuteration. The solvation effects on the relative stabilities of some representative species were also studied.

Computational Details

All the computations in the present study were performed using Gaussian 94 series of programs.[8] Geometry optimizations were carried out at HF/6-31G(d) level. Harmonic vibrational frequencies were evaluated at the same level in order to confirm the nature of the stationary points found and to account for the zero point energy (ZPE) correction. The ZPE correction was consistently scaled by the empirical factor 0.893.[9] As the correct

[⊗] Abstract published in *Advance ACS Abstracts,* November 15, 1997.

S1089-5639(97)00735-4 CCC: $14.00

description of hydrogen-bonded systems requires the inclusion of diffuse functions as well as electron correlation effects, we refined all the geometries at the MP2(full)/6-31+G(d,p) level.

To have more reliable energetics in the case of the lowest energy conformers, their total energies were computed at the G2(MP2)[10] level, which yields energies of an effective QCISD-(T)/6-311+G(3df,2p) quality. It should be pointed out that in our calculations we have used the MP2/6-31+G(d,p) geometries rather than the HF/6-31G(d) geometries as in the standard G2-(MP2) scheme.

Since as mentioned in the Introduction both the structures and relative stabilities of the enol and enethiol forms of **TMA** are quite sensitive to the level of theory employed, they constitute a suitably good benchmark case to investigate the performance of density functional theory in describing IHBs. For this purpose we have chosen the B3LYP approach, which was found[3c,11] to give results in good agreement with high-level ab initio calculations as far as the description of intermolecular hydrogen bonds is concerned. The exchange functional B3[12] is a hybrid method proposed by Becke that includes a mixture of Slater functional,[13] Becke's 1988 gradient correction,[14] and Hartree−Fock exchange. The correlation part, LYP,[15] is the gradient-corrected functional of Lee, Yang, and Parr. The basis set used for the DFT geometry optimization was 6-31G(d), while final energies were calculated with the 6-311+G(3df,2p) basis set. ZPE corrections, obtained at the same level used for the geometry optimizations, were scaled by the empirical factor 0.98.[16]

We have considered it also of interest to investigate the solvent effect on the relative stability of the most stable tautomers. The effect of solute−solvent interactions was initially taken into account by means of the self-consistent isodensity polarized continuum model (SCIPCM). In this approach the interaction between the dipole moment of the solute with the dipole induced in the surrounding medium is taken into account by enclosing the solute in a cavity defined as an isodensity surface of the molecule. This cavity is surrounded by the solvent which is considered as a uniform dielectric with a given permittivity, ϵ_r. An overview of these methods can be found in ref 17. All these calculations were performed using the B3LYP approach in order to explicitly include electron correlation effects. As for the solvent-free calculations geometry optimizations were performed using the 6-31G(d) basis set, while the final energies were obtained at the B3LYP/6-311+G(3df,2p) level. The permittivity value used ($\epsilon = 74.58$) corresponds to that of water. The main limitation of this approach is that specific solute−solvent hydrogen bonding interactions are discarded. Hence, to estimate the possible effect of these specific interactions we have used a discrete−continuum model,[18] in which the SCIPCM approach is applied to clusters formed by the interaction of the solute with a finite number of solvent molecules. Since **TMA** presents two basic centers, we have initially considered clusters with two water molecules where both basic centers are solvated. A further refinement would imply adding a third water molecule which, for the particular case of the cyclic **E1** and **T1** systems, will be able to interact with the proton involved in the IHB. A similar refinement was included in the treatment of the open-chain structures.

The nature of the IHB in the corresponding structures has been studied using the atoms-in-molecules (AIM) theory of Bader,[19] which is based on a topological analysis of the electronic charge density, ρ. By means of the AIMPAC series of programs[20] we have located the bond critical points[19] (bcp's). Further information on the relative strength of the linkage can be obtained in terms of the Laplacian, $\nabla^2\rho$, and in terms of the energy density, $H(r)$. In this context it must be mentioned that, for the particular case of O−H···O intermolecular hydrogen bonds in water and methanol clusters, a reasonably good linear correlation between the charge density at the bcp's and the strength of the HBs was reported.[21] The net atomic charges were calculated using the natural bond orbital (NBO) analysis.[22] Both AIM and NBO analysis were performed on MP2 densities to include electron correlation effects.

Results and Discussion

Relative Stabilities. Total and relative energies of the different rotamers of the enol, enethiol, and diketo tautomers of **TMA** (See Figure 1) are given in Table 1. This table includes also the results corresponding to the transition state between structures **E1** and **T1** (**TS 1/1**).

The first conspicuous fact of Table 1 is that, with the only exception being the species **E1** and **T1**, which present an IHB, the enethiol tautomers (**T2**−**8**) are about 5−10 kcal/mol more stable than the enol analogues (**E2**−**8**); that is, the structures containing S−H and C═O bonds are systematically more stable that those containing O−H and C═S bonds, instead. These differences reflect essentially the fact that a carbonyl bond is stronger than a thiocarbonyl one, while the S−H linkage is weaker than the O−H bond, the first effect being dominant. In fact, a reasonably good estimation of these stability differences can be obtained by comparing the atomization energies of [thioformaldehyde (H_2CS) + methanol (CH_3OH)] with the atomization energies of [formaldehyde (H_2CO) + thiomethanol (CH_3SH)]. From the corresponding G2 total energies,[23] it is found that the last couple of compounds have an atomization energy about 11 kcal/mol higher than the first couple of compounds. The stability differences between enol and enethiol tautomers of **TMA** given in Table 1 are clearly of the same order of magnitude.

It can also be observed that within each subset the relative stabilities of the different rotamers do not differ significantly, with the only exception being **E2**, due to the repulsions between oxygen and sulfur lone pairs. The energy ordering within both series of compounds is as follows:

$$\mathbf{T1} \approx \mathbf{T7} \approx \mathbf{T4} < \mathbf{T2} \approx \mathbf{T6} \approx \mathbf{T5} < \mathbf{T3} < \mathbf{T8}$$

$$\mathbf{E1} < \mathbf{E7} < \mathbf{E4} < \mathbf{E5} \approx \mathbf{E6} < \mathbf{E3} < \mathbf{E8} < \mathbf{E2}$$

In general, this ordering shows that, excluding the rotamers containing the IHB, the most stable structures are the ones less sterically hindered. It is also worth noting that at the MP2/6-31+G(d,p) level the relative stabilities of species **T1**, **T4**, and **T7** differ by less than 1.5 kcal/mol. Hence, the final energies for these particular cases have been recalculated at the G2(MP2) level. The results in Table 1 indicate that when higher order correlation corrections are included in the theoretical treatment, these three rotamers become even closer in energy. This is not the case however for the corresponding enol analogues. As shown in Table 1, the energy gap between structure **E1** and structure **E7**, which at the MP2/6-31+G(d,p) level is already 5.7 kcal/mol, increases slightly when obtained at the G2(MP2) level of theory.

For the diketo conformers only three rotamers are minima of the PES because structure **K1** collapses without activation barrier to structure **K3**. None of the three stable rotamers are strictly planar, since the C═O and the C═S groups lie always in different planes. It is also important to notice that diketo conformers are much less stable than the enethiol ones, as previously found by Buemi[24] at the AM1 semiempirical level.

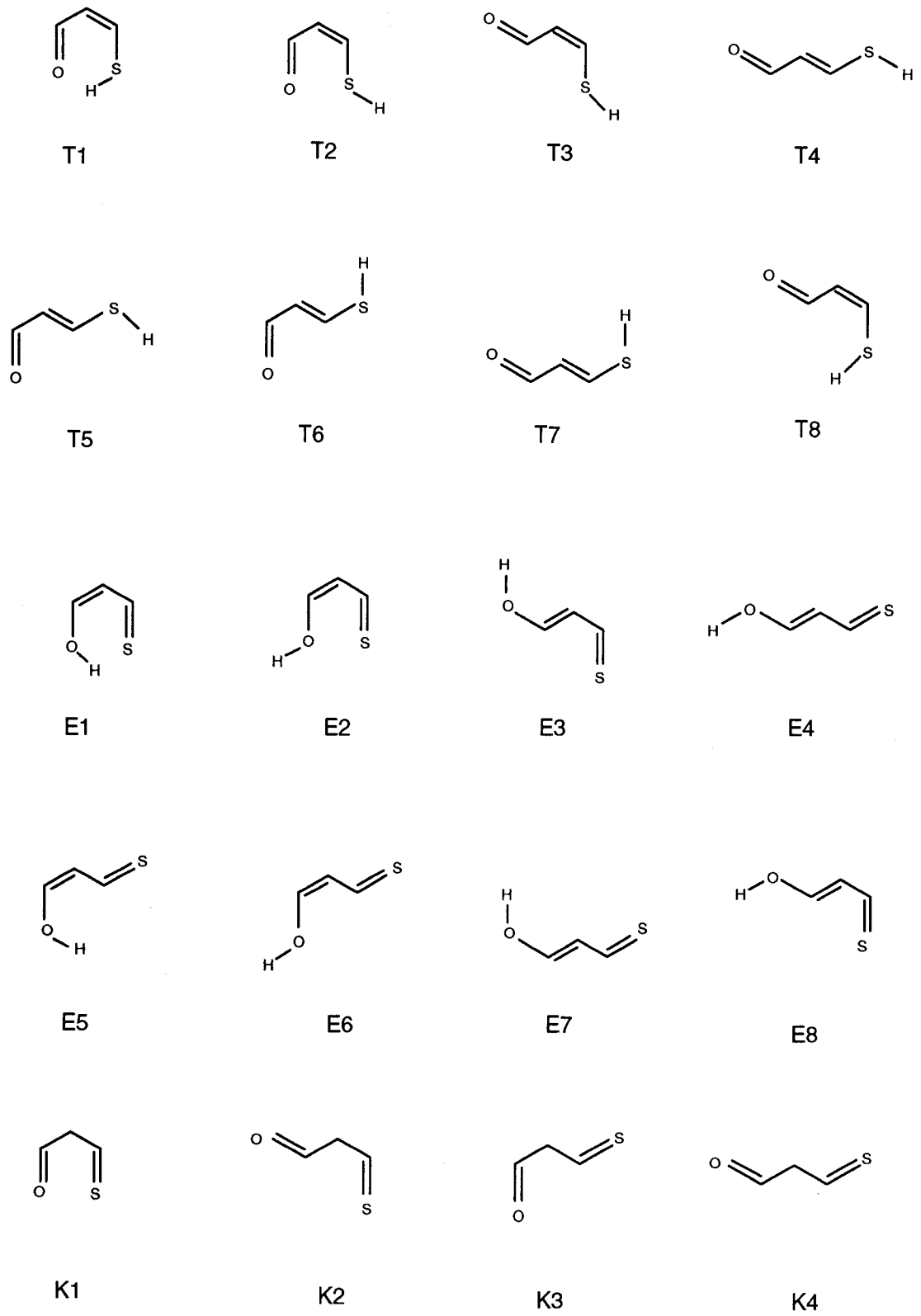

Figure 1. Schematic representation of the different enol (**E1**−**8**), enethiol (**T1**−**8**), and diketo (**K1**−**4**) tautomers of thiomalonaldehyde.

This seems to be a characteristic of this sulfur-containing compounds. In fact, although for malonaldehyde the most stable diketo form was predicted[3f] to be slightly (0.5 kcal/mol) more stable than the most stable enol form, the enol forms of dithiomalonaldehyde were predicted[25] to be more stable than the diketo ones, as in our case.

Quite interestingly, the B3LYP approach gives results very close to those obtained at the G2(MP2) level, indicating that, also at the DFT level, the structures **T1, T4**, **T7**, and **E1** are nearly degenerate in the gas phase.

Intramolecular HB and Enol−**Enethiol Tautomerism.** As mentioned above species **E1** and **T1** are practically degenerate even though, in general, enethiol tautomers are sizably more stable than their enol analogues. This is partially related to the quite different stability of the IHB present in both species. Therefore, in this section we shall try to analyze this particular problem.

The optimized geometries of both tautomers are given in Table 2. It can be observed that there are significant differences between the MP2/6-31+G(d,p) optimized structures and the HF/

TABLE 1: Total Energies in Hartrees. Values within Parentheses Are the Relative Stabilities with Respect to E1 and T1, Respectively (in kcal/mol). Values within Brackets are the Relative Stabilities of Each Enol Tautomer with Respect to the Corresponding Enethiol Analog (in kcal/mol). All Relative Energies Include Scaled ZPE Corrections. ZPE (Unscaled) in kcal/mol

	MP2/6-31+G(d,p)					G2(MP2)			B3LYP/6-311+G(3df,2p)//B3LYP/6-31G(d)					B3LYP/6-311+G(3df,2p) //B3LYP/6-31G(d) + SCIPCM			
	energy			ZPE	μ (D)[a]	energy			energy			ZPE	μ (D)	energy			ZPE
T1	−589.027725	(0.0)		42.24	3.1	−589.333755	(0.0)		−590.216574	(0.0)		39.12	2.5	−590.221509	(0.0)		39.08
				36.15[b]		−589.342419[b]											
T1ww									−743.153032			69.22	3.9	−743.166198[c]			
T1www									−819.620838			84.55	2.7	−819.636952[c]			
T2	−589.024417	(2.1)		42.24	4.2												
T3	−589.021313	(3.5)		41.63	5.1												
T4	−589.024777	(1.3)		41.59	4.9	−589.332889	(0.5)		−590.215001	(0.4)		38.50	4.4	−590.224210	(−2.3)[d]		
T4ww									−743.155786				6.8	−743.172170			
T4www									−819.619875				7.5	−819.641497			
T5	−589.023133	(2.4)		41.72	2.6												
T6	−589.023589	(2.3)		41.91	3.8												
T7	−589.025930	(0.8)		41.85	3.5	−589.333179	(0.4)		−590.215554	(0.2)		38.69	3.5	−590.224545	(−2.3)[d]		
T8	−589.020426	(4.3)		41.88	3.4												
E1	−589.028893	(0.0)	[1.3]	44.52	3.5	−589.333499	(0.0)	[0.2]	−590.219982	(0.0)	[−0.3]	41.03	2.8	−590.224164	(0.0)	[0.2]	40.98
				37.65[a]		−589.343273[b]		[−0.5][b]									
E1ww									−743.155087			70.91	2.8	−743.166029[c]			
E1www									−819.618874			70.91	2.8	−743.166029[c]			
E2	−589.009981	(11.4)	[10.6]	43.96	5.5												
E3	−589.014914	(8.4)	[7.4]	44.06	4.3												
E4	−589.016746	(7.0)	[7.0]	43.83	6.0				−590.207547	(7.5)		40.73	6.0				
E5	−589.016317	(7.5)	[4.5]	44.10	3.1												
E6	−589.015937	(7.6)	[5.4]	43.96	6.2				−590.205517	(8.8)		40.82	6.1	−590.217668	(3.9)		
E6ww									−743.151955				9.3	−743.172064			
E6www									−819.621857				9.1	−819.644604			
E7	−589.019093	(5.7)	[6.2]	44.08	3.7	−589.323928	(6.0)		−590.209479	(6.5)		40.95	3.7				
E8	−589.013852	(8.9)	[7.7]	43.91	3.5												
TS 1/1	−589.020467	(1.7)		40.51	3.4	−589.328617	(3.0)		−590.211461	(2.1)		37.64	2.5	−590.215558	(1.3)[d]		
K3									−590.202545	(9.7)		39.73	2.8	−590.207547	(9.2)[d]		
K4									−590.201933	(10.2)		39.84	2.7				

[a] Values of dipole moment correspond to HF/6-31g(d) level. [b] Values corresponding to the species where H9 is replaced by deuterium. [c] Values corresponding to the discrete-continuum solvation model. See explanation in text. [d] ZPE correction including solvent has been taken from the corresponding free solvent computation.

TABLE 2: Structural Parameters Obtained at Different Levels of Theory. Bond Distances in Angstroms, Angles in Degrees, and Rotational Constants (*A*, *B*, *C*) in Megahertz. NBO Atomic Charges Are Included for Species T1 and E1

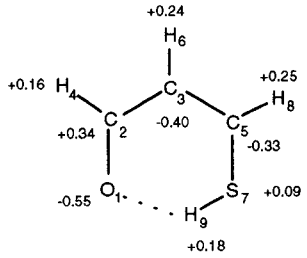

T1

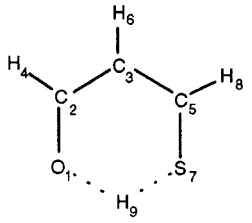

TS 1/1

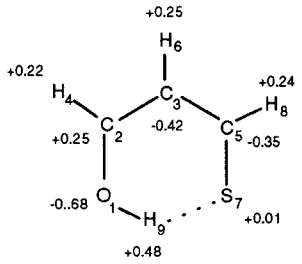

E1

	T1			TS 1/1			E1		
parameter	MP2/6-31+G(d,p)	B3LYP/6-31*	B3LYP/6-31G* SCIPCM	MP2/6-31+G(d,p)	B3LYP/6-31*	B3LYP/6-31G* SCIPCM	MP2/6-31+G(d,p)	B3LYP/6-31*	B3LYP/6-31G* SCIPCM
r(O1−C2)	1.243 (1.191)[a]	1.232	1.236	1.279	1.267	1.270	1.329 (1.300)[a]	1.314	1.316
r(C2−C3)	1.455 (1.471)	1.455	1.453	1.410	1.418	1.419	1.371 (1.352)	1.377	1.380
r(C3−C5)	1.362 (1.331)	1.358	1.358	1.386	1.382	1.379	1.426 (1.426)	1.417	1.412
r(C5−S7)	1.729 (1749)	1.741	1.743	1.689	1.713	1.720	1.654 (1.644)	1.674	1.681
r(C2−H4)	1.010 (1.093)	1.108	1.106	1.090	1.098	1.096	1.083 (1.074)	1.088	1.087
r(C3−H6)	1.083 (1.075)	1.087	1.086	1.080	1.085	1.084	1.081 (1.072)	1.086	1.085
r(C5−H8)	1.084 (1.075)	1.087	1.087	1.084	1.089	1.088	1.088 (1.078)	1.092	1.091
r(S7−H9)	1.340 (1.330)	1.362	1.359	1.526	1.550	1.547	2.043 (2.246)	2.061	2.063
r(O1−H9)	1.951 (2.153)	1.898	1.930	1.287	1.317	1.320	0.999 (0.967)	1.011	1.009
∠(O1−C2−C3)	125.3 (125.9)	126.0	126.2	124.0	124.8	124.7	125.7 (128.1)	126.4	126.1
∠(C2−C3−C5)	125.6 (126.7)	125.6	126.1	121.9	122.3	122.6	124.6 (125.7)	124.7	124.9
∠(C3−C5−S7)	129.5 (131.4)	128.5	128.5	125.0	125.1	124.8	127.5 (128.7)	127.5	127.5
∠(C5−S7−H9)	95.0 (98.5)	94.0	94.6	86.1	86.3	86.4	82.8 (82.1)	82.6	82.5
∠(O1−C2−H4)	119.0 (119.6)	119.0	119.0	116.4	116.5	116.6	112.8 (112.3)	112.7	112.9
∠(C2−C3−H6)	145.5 (115.8)	116.4	116.2	118.6	117.9	117.7	116.9 (116.5)	116.8	116.7
∠(C3−C5−H8)	118.3 (118.9)	119.1	119.2	118.5	118.7	119.0	115.4 (115.4)	115.4	115.4
∠(S7−H9−O1)	137.9	139.5	138.6	157.3	155.4	155.4	151.8 (143.9)	150.6	150.6
A	7613.05	7698.70	7694.38	7592.31	7536.08	7506.86	7703.09	7657.80	7636.70
B	3017.07	3036.39	3012.20	3510.59	3439.39	3436.76	3206.70	3171.61	3166.86
C	2172.54	2177.56	2164.74	2400.58	2361.58	2357.47	2264.16	2242.74	2238.56

[a] Values within parentheses correspond to MP2/TZP optimized structures taken from ref 6.

TABLE 3: Relative Stabilities of the Structures T1, E1, and TS1/1, at Different Levels of Theory (in kcal/mol) Including Scaled ZPE Corrections. Values within Parentheses Do Not Include ZPE Corrections

method	T1		TS1/1		E1	
HF/6-31G(d)	0.0	(0.0)	14.5	(16.0)	4.5	(2.5)
MP2(full)/6-31+G(d,p)	0.0	(0.0)	3.0	(4.6)	1.3	(−0.7)
MP2/6-311+G(3df,2p)	0.0	(0.0)	1.7	(3.3)	−0.2	(−2.2)
G2(MP2)	0.0	(0.0)	3.2	(4.8)	0.2	(−1.8)
G2(MP2) deuterated	0.0	(0.0)			−0.5	(−1.8)
B3LYP/6-311+G(3df,2p)	0.0	(0.0)	1.8	(3.2)	−0.3	(−2.1)
B3LYP/6-311+G(3df,2p) + SCIPCM	0.0	(0.0)	2.3	(3.7)	0.2	(−1.7)

TABLE 4: Bonding Characteristics: Charge Density, ρ; Laplacian of the Charge Densities, $\nabla^2\rho$; and Energy Density, $H(r)$. All Values in Atomic Units

	T1			TS1/1			E1		
bond	ρ	$\nabla^2\rho$	$H(r)$	ρ	$\nabla^2\rho$	$H(r)$	ρ	$\nabla^2\rho$	$H(r)$
O1−C2	0.415	0.535	−0.705	0.345	−0.022	−0.573	0.308	−0.169	−0.493
C2−C3	0.278	−0.730	−0.257	0.307	−0.856	−0.315	0.326	−0.925	−0.359
C3−C5	0.325	1.018	0.399	0.314	−0.864	−0.330	0.294	−0.780	−0.288
C5−S7	0.202	−0.411	−0.171	0.217	−0.369	−0.260	0.224	−0.125	−0.278
C2−H4	0.290	−1.091	−0.316	0.291	−1.117	−0.318	0.296	−1.157	−0.329
C3−H6	0.288	−1.060	−0.317	0.285	−1.044	−0.311	0.285	−1.039	−0.310
C5−H8	0.294	−1.121	−0.328	.0289	−1.091	−0.317	0.288	−1.076	−0.313
S7−H9	0.229	−0.696	−0.327	0.146	−0.255	−0.102	0.041	0.06	−0.007
O1−H9	0.020	0.059	−0.000	0.144	−0.112	−0.116	0.323	−1.814	−0.537

TZP values reported before in the literature, in particular as far as the parameters involved in the IHBs are concerned. However, the agreement between MP2 and B3LYP optimized values is fairly good and the corresponding rotational constants (See Table 2) differ by 1% on average. Table 2 contains also the optimized geometry of the transition state (**TS1/1**) connecting both species. The optimized geometries for the remaining rotamers are available from the authors upon request.

The effect of the level of calculation on the relative stabilities of these three species is illustrated in Table 3. Two important conclusions can be drawn: (i) electron correlation effects are very significant and (ii) the ZPE corrections play a crucial role. Disregarding the ZPE corrections, the *Z*-enethiol tautomer **T1** is clearly more stable than the *Z*-enol one **E1** at the HF level, but the inclusion of electron correlation effects at the MP2 level reverses the stability order and the enol form is predicted to be more stable. The same situation is found also at higher levels, such as G2(MP2) or B3LYP/6-311+G(3df,2p). Hence, if only the final electronic energies are considered, the **E1** form is predicted to be about 2.0 kcal/mol more stable than **T1**. However, because the ZPE corrections for the enol forms are 2.0−3.0 kcal/mol systematically larger than for the enethiols, the inclusion of the ZPE correction reduces the gap drastically or even changes the stability order. These differences in the ZPE corrections reflect essentially the large frequency difference between typical O−H stretching modes, which are observed around 3600 cm^{-1}, and the S−H stretching displacements usually observed around 2600 cm^{-1}. A similar finding has been reported in the literature[26] regarding the thiol−thione tautomerism in mercaptopyridines, diazinethiones, and related compounds. The most important consequence is that, at the G2(MP2) level, **T1** is predicted to be only slightly more stable than its enol analogue **E1**. Since the energy gap between **E1** and **T1** is really small, we have checked what would be the effect of replacing the hydrogen atom involved in the IHB by deuterium. The result is that the difference between the ZPEs of both species decreases by about 0.7 kcal/mol, so our G2(MP2) estimations predict that when dealing with the deuterated species, the **E1** tautomer should be slightly more stable than its thiol analogue **T1**.

The small energetic gap between species **E1** and **T1** was suggested[6] to be a direct consequence of the stronger IHB of the former. A topological analysis of the charge density of both **E1** and **T1** is consistent with this idea. The charge density at the HB critical point of structure **E1** is twice that calculated for species **T1** (see Table 4) and the energy density is slightly negative rather than zero, which indicates a stabilizing charge concentration in that region. These differences reflect substantial dissimilarities in the charge distribution of both species mostly related to the differences between the electronegativities and polarizabilities of sulfur and oxygen atoms. In **T1** the hydrogen atom involved in the IHB has a quite small positive charge, while the same hydrogen in species **E1** exhibits a substantially higher positive charge (see scheme in Table 2). Furthermore, while in tautomer **E1** this hydrogen atom interacts with a sulfur atom, which is very polarizable, in species **T1** it interacts with an oxygen atom much more difficult to polarize.

Another index closely related with the relative strengths of both HBs is the shiftings of the O−H and S−H stretching frequencies. It is well established that the stronger the HB, the larger is this shifting. To estimate this effect, we need a reference system where the HB is absent and which presents an electronic structure similar to that of the hydrogen-bonded species. Following the arguments of Craw and Bacskay,[7] the most suitable candidates are rotamers **E7** and **T7**. Our calculations at the B3LYP/6-31G(d) level (see Table 5) indicate that the S−H stretching frequency for the **T1** tautomer appears red-shifted by ca. 160 cm^{-1} with respect to that in **T7**, while the red-shifting of the O−H stretch of **E1** with respect to **E7** is 759 cm^{-1}. This implies that while in all enol tautomers the highest vibrational frequency (around 3600−3700 cm^{-1}) corresponds always to the O−H stretch, this is not the case for **E1**, where the C−H stretches appear at higher frequencies than the O−H stretch (see Table 5). These findings are also consistent with the lengthening of the S−H and O−H linkages on going from **T7** and **E7** species to **T1** and **E1**, respectively. In the first case the S−H bond elongates by 0.011 Å, while in the second case the elongation of the O−H bond is 0.026 Å. For both cyclic tautomers **E1** and **T1** the lowest vibrational frequency corresponds to the stretching of the IHB (see Table 5). In agreement with our previous arguments, the larger value corresponds to **E1**, which is the system that presents the stronger HB.

There is however a second factor which enhances the stability of species **E1**, associated with a typical resonance-assisted hydrogen-bonding (RAHB) mechanism.[27] The values of the

TABLE 5: Harmonic Vibrational Frequencies at the B3LYP/6-31g(d) Level (in cm^{-1})

T1		E1	
ν	assignment	ν	assignment
218	stretch. O−H9	249	stretch. S−H9
221	bending C2−O out of plane	255	bending C5−S out of plane
369	bending C2−C3−C5 out of plane	407	bending C2−C3−C5 out of plane
404	bending C3−C2−O + bending C3−C5−S	421	bending O−C2−C3, C3−C5−S, in plane
565	bending S−H9 out of plane	778	bending C2−H4, C3−H6, C5−H8, in face
731	stretch. C5−S	807	bending C2−C3−C5 + stretch. C5−S
737	bending C2−H4, C3−H6, C5−H8, in phase, out of plane	848	bending O−H9 out of plane
807	bending C2−C3−C5 in plane	874	bending S−C5−C3
975	bending C5−H8, C3−H6, out of ;lane, out of phase	953	bending C2−H4, C3−H6, out of phase, out of plane
988	bending H9−S−C5 + stretch. C2−C3	1013	bending C2−H4 out of plane
1014	bending H9−S−C5 − stretch. C2−C3	1069	bending O−C2−C3 + stretch. C5−S
1032	bending C2−H4 out of plane	1213	stretch. C3−C5, C5−S
1239	stretch. C3−C5	1319	bending C2−H4 + stretch. C2−O
1413	bending C2−H4, C3−H6, C5−H8, in phase, in plane	1393	ring deformation out of plane
1455	bending C2−H4, C5−H8, out of phase + stretch. C2−O	1455	bending C2−O−H9 + stretch. C2−C3
1590	stretch. C3−C5, C2−C3, out of phase	1518	stretch. C3−H5 + C2−O
1738	stretch. C2−O	1641	stretch. C2−C3 + C2−O
2519[a]	stretch. S−H9	2949[b]	stretch. O−H9
2961	stretch. C2−H4	3131	stretch. C5−H8
3183	stretch. asym. C3−H6, C5−H8	3192	stretch. asym. C2−H4, C3−H6
3201	stretch. sym. C3−H6, C5−H8	3212	stretch. sym. C2−H4, C3−H6

[a] The value of the stretching S−H9 for **T7** rotamer is 2686 cm^{-1}. [b] The value of the stretching O−H9 for **E7** rotamer is 3708 cm^{-1}.

charge densities at the bcp's given in Table 4 reveal that the existence of an IHB in **E1** favors a significant delocalization of charge within the cyclic structure. A much smaller charge delocalization takes place in the case of **T1** form. Actually, in tautomer **E1** the charge densities at the C2−C3 and C3−C5 bonds are more similar than in **T1**, and accordingly the corresponding bond lengths are also closer. This is easily understood by looking at the evolution of the charge density on going from the thienol **T1** to the enol **E1** through the transition state (**TS1/1**). In species **T1**, due to the large electron affinity of the oxygen atom and the fact that the carbonyl group is very difficult to perturb, a quite localized structure with alternate double and single bonds is strongly favored. When the hydrogen atom moves closer to the oxygen, there is a significant charge transfer from the latter to the former, to finally form a O−H covalent bond. This charge transfer enhances the electronegativity of the oxygen atom, which withdraws charge from the C−O linkage. This results in a polarization of the carbonyl carbon, which is transmitted along the C−C−C chain of bonds and favored by the fact that S is only somewhat electronegative and highly polarizable. The result is a significant charge delocalization in the C2−C3−C5−S moiety, which enhances the stability of the **E1** form. This also explains why the gap between **E1** and the open-chain structure **E4** (or **E7**) is much higher than that found between species **T1** and **T4** (or **T7**).

We have also estimated the energy barrier for the **E1** → **T1** tautomerization to be 3.2 kcal/mol at the G2(MP2) level, with respect to **T1**. It is important to emphasize that electron correlation effects have a dramatic influence on the height of the barrier. As illustrated in Table 3, the inclusion of correlation effects decreases the barrier by a factor of 5. As expected the influence of ZPE corrections is to decrease the barrier. It is also worth noting that although the relative stabilities of the different minima obtained at the B3LYP/6-311+G(3df,2p) level are in fairly good agreement with the corresponding G2(MP2) estimates, in the case of the transition state **TS1/1** this agreement is worse. As a consequence, the tautomerization barrier at the B3LYP/6-311+G(3df,2p) level is predicted to be only 1.8 kcal/mol. The potential energy curve corresponding to the hydrogen-transfer process, evaluated at the MP2/6-31+G(d,p) level, has been plotted in Figure 2. In this figure we have chosen as suitable reaction coordinate the O_1-H_9 distance, and all the remaining geometrical parameters were fully optimized. As expected, the potential energy curve presents two nonequivalent wells. While the potential on going from **E1** to **T1** is very steep, the evolution from **T1** to **E1** is much smoother. In the first case these characteristics are the consequence of the three factors mentioned above: (i) it is necessary to break a O−H bond which is stronger than the S−H bond to be formed, (ii) it is necessary to break an IHB stronger than the one to be formed, and (iii) both processes i and ii lead to a smaller electron charge delocalization within the system.

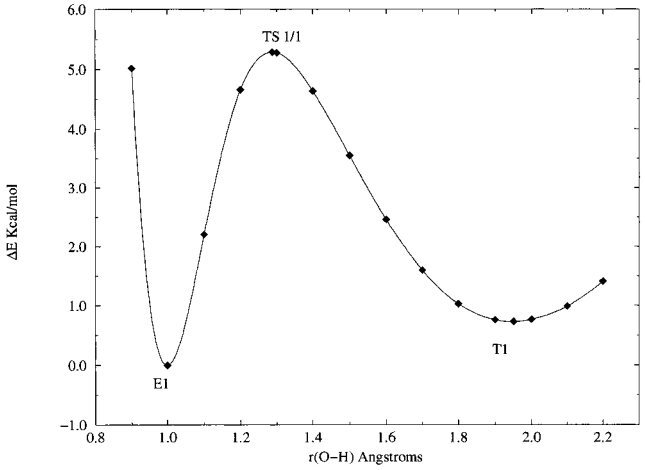

Figure 2. Potential energy curve for the **E1** → **T1** tautomerism. Values are obtained at the MP2(full)/6-31+G(d,p) level.

Solvation Effects. *Continuum Model*. The geometries of the systems studied do not change appreciably when solvent effects are taken into account using exclusively a continuum model (see Table 2). Similarly solute−solvent interactions imply negligible changes in the ZPEs of species **E1** and **T1** (see Table 1). Hence, for the sake of economy, the values of the ZPEs used for the solvated forms of species **T4**, **T7, E6, K3,** and **TS1/1** were those calculated before for the unsolvated systems. Solvation effects on the relative stabilities are however more significant. As shown in Table 1, solute−solvent interactions do not affect significantly the relative stabilities of the

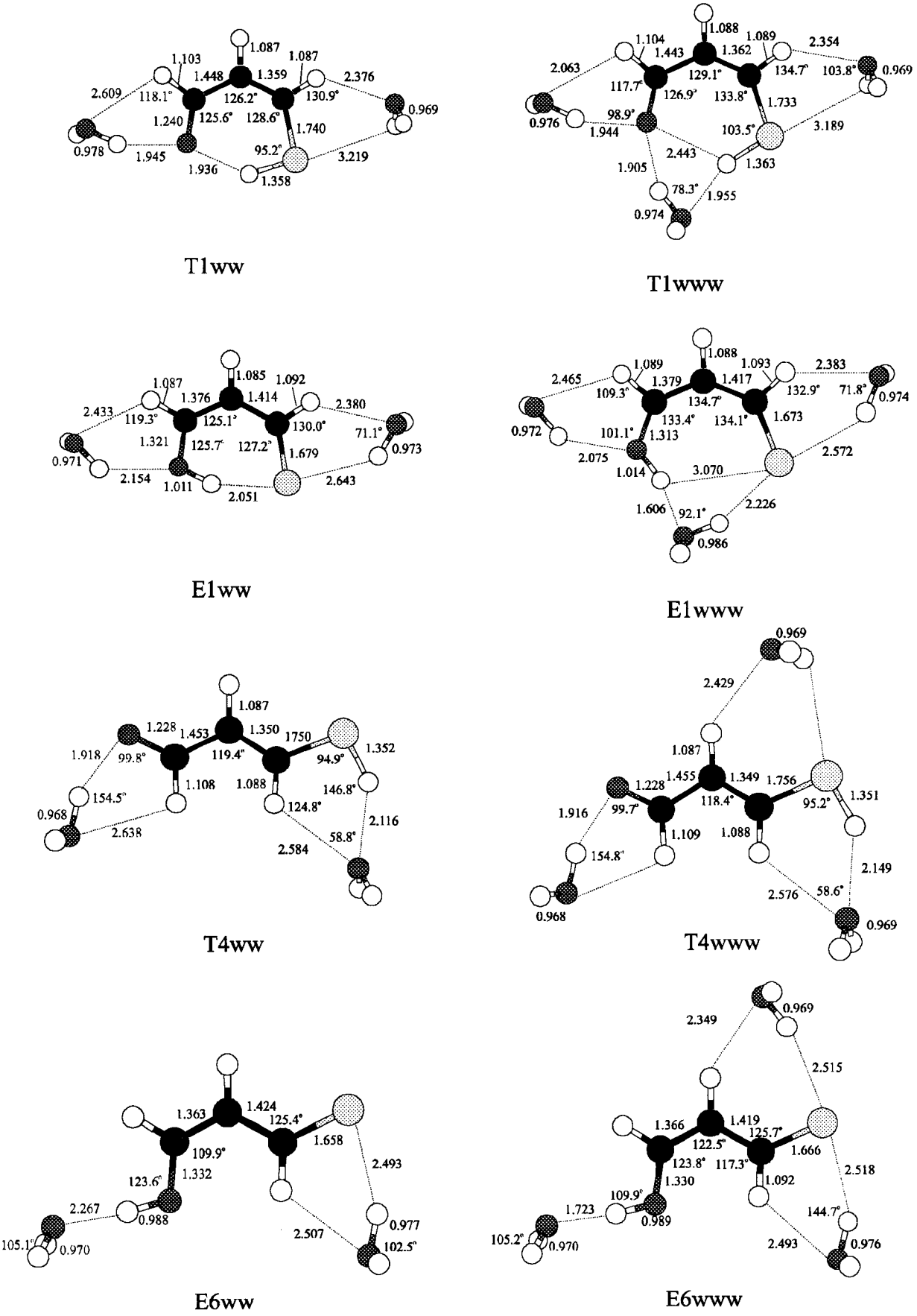

Figure 3. B3LYP/6-31G* optimized geometries for the clusters **T1**, **E1**, **T4**, and **E6** with two and three water molecules. Bond distances in angstroms and bond angles in degrees.

cyclic hydrogen-bonded species **E1** and **T1**, which remain almost degenerate in aqueous solution. In contrast, the open-chain rotamers **T4** and **T7** become sizably stabilized.

The enhanced stability of forms **T4** and **T7** with respect to **T1** has a double origin; on one hand, the open-chain species have a larger dipole moment (4.4 and 3.5 D, respectively, at

TABLE 6: Relative Stabilities of the Clusters with Two and Three Water Molecules Calculated at the B3LYP/ 6-311+G(3df,2p) Level Including Scaled ZPE Corrections

	ΔE			ΔE	
	discrete	discrete-continuum		discrete	discrete-continuum
T1ww	2.4	4.3	**T1www**	0.1	3.5
E1ww	2.7	6.1	**E1www**	3.4	7.7
T4ww	0.0	0.0	**T4www**	0.0	0.0
E6ww	4.5	2.1	**E6www**	1.3	0.7

the B3LYP/6-311+G(3df,2p) level) than the cyclic one (2.5 D), and on the other hand they interact in a more efficient way with the solvent. This is also the case for **E6** and **K3** species. However, despite the large dipole moment of the former, it still lies higher in energy than the most stable enethiols. Although diketo tautomers seem to have been detected in other thiocarbonyl-containing compounds such as thioacetylacetone,[2] the diketo conformers of **TMA** are predicted to be the least stable in aqueous solution, because their dipole moments are smaller than those of the enethiols and enols (see Table 1). It can also be observed that the **E1**−**T1** tautomerization barrier increases slightly when solvation effects are included (see Table 3).

Specific Solute−*solvent interactions.* To investigate whether specific solute−solvent hydrogen-bonding interactions are significantly important regarding the relative stabilities of **TMA** conformers, we have chosen as a representative set **E1, T1, T4,** and **E6,** the former two because they are the most stable conformers in the gas phase, while **T4** is, among the most stable enethiol isomers, the one with the highest dipole moment. Similarly **E6** is the most polar enol tautomer.

The optimized geometries of the solvation clusters of these species with two and three water molecules, namely, **E1ww, T1ww, T4ww, E6ww, E1www, T1www, T4www**, and **E6www**, have been schematized in Figure 3. Their total energies have been included in Table 1. Both the optimized geometries and the relative energies (see Table 6) put in evidence nonnegligible specific solvation effects, particularly for clusters involving three water molecules. Actually, the interaction with only two molecules does not change the degeneracy of tautomers **E1** and **T1**, because the two water molecules solvating both heteroatoms behave as hydrogen bond acceptors and do not affect significantly the IHB. This is not the case for tautomer **T4**, where the water attached to the carbonyl group behaves as a hydrogen bond donor, while that interacting with the thiohydroxyl group behaves as a hydrogen bond acceptor. As a consequence, **T4** becomes particularly stabilized and the cluster **T4ww** is the global minimum. The interactions with the enol tautomer **E6** are similarly strong, but not enough to counterbalance the low stability of this species. The result is that **E6ww** and **T1ww** clusters are still ca. 2 and 4.5 kcal/mol less stable than **E1ww** and **T4ww**, respectively.

The interaction with a third water molecule changes the situation significantly in the sense that the **E1** and **T1** tautomers are not degenerate anymore. The third water molecule, which behaves as a HB acceptor, interacts essentially with the proton involved in the IHB, which is significantly perturbed. However, this perturbation is larger for **E1** than for **T1** because the OH group of **E1** is a better HB donor than the SH group of **T1** (see Figure 3). Furthermore, in the **E1www** cluster, the IHB has practically disappeared since the hydroxyl group prefers to form a HB with the third water molecule than with the sulfur atom of the thiocarbonyl group because the former is a better HB acceptor than the latter. As a consequence, the **E1** moiety becomes sizably destabilized and **E1www** is predicted to be 3.3 kcal/mol less stable than **T1www**.

The interaction with a third water molecule contributes to further stabilize the open-chain enethiol **T4** and enol **E6** forms**.** In this respect it should be noted that although **T4www** is predicted to be the most stable cluster, it is practically degenerate with **T1www**. As we shall discuss in the next section, this situation will change when including bulk effects.

Discrete−*Continuum Model.* The relative stabilities of the different clusters discussed in the previous section change significantly when the interactions with the surrounding medium are taken into account through the use of a SCIPCM approach. It is important to emphasize that the unsolvated systems with larger dipole moments lead also to the most polar water clusters. Actually, while the water clusters of **E1** and **T1** have dipole moments slightly smaller than the unsolvated systems, for **T4** and **E6** it is the other way around. The important consequence is that while the **T1www** and **T4www** clusters are degenerate in the gas phase, the latter becomes significantly stabilized in solution, and therefore neither chelated enol nor chelated enethiol forms should be present in condensed media. Also importantly, due to the large dipole moment of the enol cluster **E6www**, the discrete−continuum model predicts it to be very close in energy to the global minimum, **T4www**.

In summary, we may conclude that when discrete and continuum solute−solvent interactions are taken into account, the most stable species are the open-chain enethiols and enols. It should be noted, however, that previous PMR studies on some monothio-β-diketones showed[28] that enethiol forms were absent in solvents of low dielectric constants, while the hydrogen-bridged cis-enol form predominates in fast equilibrium with nonchelated enol forms.

Conclusions

From the results discussed in previous sections we can conclude that in general the enethiol tautomers of **TMA** are 5−10 kcal/mol more stable than the corresponding enol analogues, with the only exception being the hydrogen-bonded species **T1** and **E1**, which are the global minima of both series. At the G2(MP2) level both species are nearly degenerate, the enethiol **T1** being 0.2 kcal/mol more stable than the enol **E1**. Our theoretical models indicate that electron correlation effects stabilize preferentially the enol form, while the ZPE corrections work in the opposite direction, due essentially to the differences between S−H and O−H stretching frequencies. As a consequence, when the hydrogen atom involved in the IHB of both tautomers is replaced by deuterium, the stability order is reversed and **E1** is predicted to be 0.5 kcal/mol more stable than **T1**. An analysis of these IHBs in terms of the topological characteristics of the electron charge density and of the shifts of the S−H and O−H vibrational frequencies reveals that the HB in species **E1** is much stronger than in structure **T1**. The existence of this IHB results in an increase of the electron delocalization, which enhances the stability of tautomer **E1,** in a typical RAHB mechanism. Importantly, at the G2(MP2) level two open-chain rotamers, namely **T4** and **T7**, are predicted to be within an energy gap smaller than 0.5 kcal/mol with respect to the global minimum.

Specific solute−solvent hydrogen-bonding interactions have nonnegligible effects on the structure of the systems investigated, in particular on the species presenting an IHB. These effects are apparent when at least three solvent molecules are taken into account, because the third solvent molecule interacts specifically with the proton involved in the IHB. The most important consequence is that the two most stable gas-phase enol and enethiol forms, **E1** and **T1**, are not degenerate, the **T1www** cluster being 3.3 kcal/mol more stable than the

E1www. When both discrete and continuum interactions are included in the model, the open-chain enethiol **T4** is predicted to be the global minimum. However, due to the fact that the clusters of the enol **E6** with water molecules are extremely polar, this species, which is of low stability in the gas phase, in solution lies only 0.7 kcal/mol above the global minimum.

It is also important to emphasize that B3LYP/6-311+G(3df,-2p) relative stabilities are in excellent agreement with G2(MP2) values. Hence, we may conclude that density functional theory approaches might be a good alternative to high-level ab initio calculations not only for the treatment of intermolecular[11] but also for intramolecular hydrogen bonds.

Acknowledgment. This work has been partially supported by the D.G.I.C.Y.T. Project No. PB93-0142-C03-02. L.G. acknowledges a grant from the Ministerio de Educación y Cultura. We would like to thank one of our referees for helpful criticism.

References and Notes

(1) See, for instance: Schuster, P.; Zundel, G.; Sandorfy, C. The Hydrogen Bond. North-Holland, New York, 1976. Buckingham, A. D.; Powler, P. W.; Hutson, J. M. Chem. Rev. **1988**, *88*, 963. Curtiss, L. A.; Blander, M. *Chem. Rev. (Washington, D.C.)* **1988**, *88*, 827. Hibbert, F.; Emsley, J. Hydrogen Bonding and Chemical Reactivity. *Adv. Phys. Org. Chem*. **1990**, *26*, 255. Jeffrey, G. A. *An Introduction to Hydrogen Bonding*, Oxford University Press: New York, 1997.

(2) For a discussion, see: Emsley, J. *Structure and Bonding*; Springer-Verlag: Berlin, 1984.

(3) See for instance: (a) Frisch, M. J.; Scheiner, A. C.; Schaefer, H. F., III; Binkley, J. S. *J. Chem. Phys.* **1985**, *82*, 4194. (b) Buemi, G. *J. Mol. Struct*. **1990**, *208*, 253. (c) Sim, F.; St-Amant, A.; Papai, I.; Salahub, D. R. *J. Am. Chem. Soc.* **1992**, *114*, 4391. (d) Latajka, Z.; Scheiner, S. *J. Phys. Chem*. **1992**, *96*, 9764. (e) Chiavassa, T.; Verlarque, P.; Pizzala, L.; Allouche, A.; Roubin, P. *J. Phys. Chem.* **1993**, *97*, 5917. (f) Mulhearn, D. C.; Bachrach, S. *J. Org. Chem.* **1995**, *60*, 7110. (g) Barone, V.; Adamo, C. *J. Chem. Phys.* **1996**, *105*, 11007.

(4) See, for instance: Redington, R. L.; Redington, T. E. *J. Mol. Struct.* **1979**, *78*, 229. Redington, R. L. *J. Chem. Phys*. **1990**, *92*, 6447. Ríos, M. A.; Rodríguez, *Can. J. Chem.* **1991**, *69*, 201. Redington, R. L.; Bock, C. W. *J. Phys. Chem*. **1991**, *95*, 10284. Sanna, N.; Ramondo, F.; Bencivenni, L. *J. Mol. Struct.* **1994**, *318*, 217. Vener, M. V.; Scheiner, S., Sokolov, N. D. *J. Chem. Phys.* **1994**, *11*, 9755. Takada, S.; Nakamura, H. *J. Chem. Phys.* **1995,** *102*, 3977. *Non-Benzenoid Conjugated Carbocyclic Compounds*; Elsevier: 1984. Mó, O.; Yañez, M.; Esseffar, M.; Herreros, M.; Notario, R.; Abboud, J. L−M. *J. Org. Chem.* **1997**, *62*, 3200, and references therein.

(5) Millefiori, S; Millefiori, A. *J. Chem. Soc., Faraday Trans. 2* **1989**, *85*, 1465.

(6) Millefiori, S; Di Bella, S. A. *J. Chem. Soc., Faraday Trans.* **1991**, *87*, 1297.

(7) Craw, J. S.; Bacskay, G. B. *J. Chem. Soc., Faraday Trans.* **1992**, *88*, 2315.

(8) Frisch, M. J.; Trunks, G. W.; Schlegel, H. B.; Gill, P. M. W.; Johnson, B. G.; Robb, M. A.; Cheeseman, J. R.; Keith, T. A.; Peterson, G. A.; Montgomery, J. A.; Raghavachari, K.; Al-Laham, M. A.; Zakrzewski, V. G.; Ortiz, J. V.; Foresman, J. B.; Ciolowski, J.; Stefanow, B. B.; Nanayaklara, A.; Challacombe, M.; Peng, C. Y.; Ayala, P. Y.; Chen, W.; Wong, M. W.; Andres, J. L.; Replogle, E. S.; Gomperts, R.; Martin, R. L.; Fox, D. J.; Binkley, J. S.; Defrees, D. J.; Baker, J.; Stewart, J. P.; Head-Gordon, M.; González, C.; Pople, J. A. *GAUSSIAN 94* (Rev. B.1); Gaussian, Inc.: Pittsburgh, PA, 1995.

(9) Pople, J. A.; Schlegel, H. B.; Krishman, R.; Defress, D. J.; Binkley, J. S.; Frisch, M. J.; Whiteside, R. A.; Hout, R. F.; Hehre, W. J. *Int. J. Quantum Chem. Symp.* **1981**, *15*, 269.

(10) Curtiss, L. A.; Carpenter, J. E.; Raghavachari, K.; Pople, J. A. *J. Chem. Phys.* **1992**, *96*, 9030.

(11) See for instance: Kim. K.; Jordan, K. D. *J. Phys. Chem.* **1994**, *98*, 10089. Latajka, Z.; Bouteiller, Y. *J. Chem. Phys.* **1994**, *101*, 9793. Zhang, Q.; Bell, R.; Truong, T. N. *J. Phys. Chem*. **1995**, *99*, 592. Del Bene, J. E.; Person, W. B.; Szczepaniak K. *J. Phys. Chem*. **1995**, *99*, 10705. Novoa, J. J.; Sosa, C. *J. Phys. Chem*. **1995**, *99*, 15873. González, L.; Mó, O.; Yáñez, M.; Elguero, J. *J. Mol. Struct. (THEOCHEM)* **1996**, *371*, 1. Barone, V.; Adamo, C. *Int. J. Quantum Chem. **1997**, 61*, 429. González, L.; Mó, O.; Yáñez, M. *J. Comput. Chem.* **1997**, *18*, 1124.

(12) Becke, A. D. *J. Chem. Phys.* **1993**, *98*, 5648.

(13) Slater, J. C. *Quantum Theory of Molecules and Solids, Vol. 4, The Self-Consistent Field of Molecules and Solids;* McGraw-Hill: New York, 1974.

(14) Becke, A. D. *J. Chem. Phys.* **1988**, *88*, 1053.

(15) Lee, C.; Yand, W.; Parr, R. G. *Phys. Rev. B* **1988**, *37*, 785.

(16) Bauschlicher Jr, C. W. *Chem. Phys. Lett*. **1995**, *246*, 40.

(17) Tomasi, J.; Persico, M. *Chem. Rev. (Washington, D.C.)* **1994**, *94*, 2027.

(18) See for instance: Pardo, L.; Osman, R.; Weisstein, H.; Rabinowitz, J. R. *J. Am. Chem. Soc.* **1993**, *115*, 8263. Tunon, I.; Rinaldi, D.; Ruiz-López, M. F.; Rivail, J. L. *J. Phys. Chem.* **1995**, *99*, 3798. Tortonda, F. R.; Pascual-Ahuir, J. L.; Silla, E.; Tunon, I. *Chem. Phys. Lett.* **1996**, *260*, 21.

(19) Bader, R. F. W.; Essen, H. *J. Chem. Phys.* **1984**, *80*, 1943. Bader, R. F. W.; MacDougall, P. J.; Lau, C. D. H. *J. Am. Chem. Soc*. **1984**, *106*, 1594. R. F. W. Atoms and Molecules. A Quantum Theory, Clarendon Press: Oxford, U.K., 1990.

(20) The AIMPAC programs package has been provided by J. Cheeseman and R. F. W. Bader.

(21) Mó, O.; Yáñez, M.; Elguero, J. *J. Chem. Phys.* **1992,** *97*, 6628. Mó, O.; Yáñez, M.; Elguero, J. *J. Mol. Struct. (THEOCHEM)* **1994**, *314*, 73.

(22) Weinhold, F.; Carpenter, J. E. *The Structure of Small Molecules and Ions*; Plenum: New York, 1988; p 227, and references therein.

(23) Curtiss, L. A.; Raghavachari, K.; Trucks, G. W.; Pople, J. A. *J. Chem. Phys.* **1991**, *94*, 7221.

(24) Buemi, G. *J. Chem. Soc., Faraday Trans.* **1990**, *86* (16), 2813.

(25) Buemi, G. *J. Mol. Struct. (THEOCHEM)* **1992,** *252*, 243.

(26) See for intance: Nowak, M. J.; Lapinski, L.; Rostkowska, H.; Les, A.; Adamowicz, L. *J. Phys. Chem*. **1990**, *94*, 7406. Nowak, M. J.; Lapinski, L; Fulara, J.; Les, A.; Adamowicz, L. *J. Phys. Chem*. **1991**, *95*, 2404. Lapinski, L.; Nowak, M. J.; Fulara, J.; Les, A.; Adamowicz, L. *J. Phys. Chem.* **1992**, *96*, 6250. See also: Molina, M. T.; Yañez, M.; Mó, O.; Notario, R.; Abboud, J.-L. M. *The Chemistry of Doubled-Bonded Functional Groups.* Supplement A3; Patai, S., Ed.; John Wiley & Sons Ltd.: New York, 1997; and references therein.

(27) Gilli, G.; Belluci, F.; Ferretti, V.; Bertolasi, V. *J. Am. Chem. Soc.* **1989**, *111*, 1023.

(28) Klose, G.; Lochmann, R.; Ludwig, E.; Uhlemann, E. *J. Mol. Struct.* **1981**, *72*, 281.